

Turbulence wave number spectra reconstruction from radial correlation reflectometry data at FT-2 tokamak

A.B. Altukhov^{1,2}, **A.D. Gurchenko**^{1,2}, **E.Z. Gusakov**^{1,2}, **N.V. Kosolapova**^{1,2,3}, **S. Leerink**⁴,
L.A. Esipov^{1,2}

¹*Ioffe Institute, St. Petersburg, Russia*

²*RLPAT, SPbSPU, St. Petersburg, Russia*

³*Institut Jean Lamour, UMR 7198 Univ. Henri Poincaré, P2M Faculté des Sciences, P70239,
F-54506 Vandoeuvre Cedex, France*

⁴*Euratom-Tekes Association, Aalto University, Espoo, Finland*

The drift wave turbulence is considered nowadays as the main source of the anomalous transport of heat and particles in magnetic fusion devices. Radial correlation reflectometry (RCR) is a microwave backscattering technique for measuring the properties of turbulent electron density fluctuations in tokamaks. The coherence decay of two scattering signals with growing probing frequency difference (Δf) is studied by the diagnostic to determine the correlation length. Commonly it is supposed that the distance between cutoffs at which the correlation of two reflectometry signals is suppressed is equal to the turbulence correlation length, however this assumption is not correct both in linear regime of RCR, where the signal correlation length appears to be larger [1, 2] and in the nonlinear regime of strong phase modulation where it appears to be smaller than the turbulence correlation length [3, 4]. Recently a new theoretical approach has been proposed [5], elucidating the way of the turbulence spectrum determination from the RCR data in the linear regime. It was shown that the turbulence radial wave number (κ) spectrum can be expressed in terms of the normalized RCR cross-correlation function (CCF) using the integral transformation

$$n_\kappa^2 \sim \frac{2}{\sqrt{\pi}} \exp\left(i \frac{\pi}{2} (sign(\kappa) + 1)\right) \frac{|\kappa|}{erf^* \sqrt{i\kappa L_0}} \int_{-\infty}^{+\infty} CCF(\Delta L) \exp(i\kappa\Delta L) d\Delta L \quad (1)$$

where ΔL is the distance between cutoff points for probing frequencies difference (Δf) and $erf^* \sqrt{i\kappa L_0}$ stands for the error function. The relation (1) obtained in [5] is typical for local diagnostics which however measure directly not the density fluctuations, but the scattering signal and therefore possess efficiency dependent on the fluctuation wave number. (Compare to enhanced microwave backscattering (BS) diagnostics in the UHR [6, 7].) The factor $|\kappa|$ in

(1) stands for the inverse scattering efficiency which possesses singularity at small radial wave numbers. This singularity in 1D model developed in [5] saturates at very small $\kappa \sim L^{-1}$ however, as the 2D slab model [8] shows the saturation condition may be less extreme

$$\kappa \simeq \frac{L}{\rho^2} \left(\frac{cq}{\omega} \right)^2, \text{ where } \rho \text{ is the beam half waist and } q \text{ stands for the poloidal wave number of}$$

fluctuation responsible for the generation of reflectometry scattering signal. Numerical simulations proving the applicability of the method presented in [9] show that RCR is able, in principle, to provide information on plasma density turbulence: the κ -spectrum and the correlation length (l_c).

The present paper presents results of the proposed method application to extract turbulence characteristics from experimental data obtained by the RCR scheme utilizing Ka and V band probing at the FT-2 tokamak ($R = 55$ cm, $a = 7.9$ cm, $B_t = (1.8\text{-}2.1)$ T, $I_p = 19$ kA,

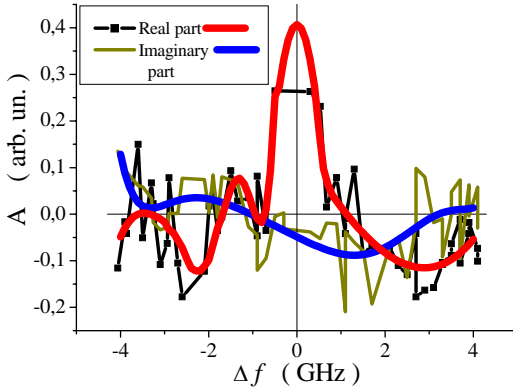


Fig. 1. CCF real and imaginary parts. The obtained real (red) and imaginary (blue) parts of the CCF are shown in Fig. 1 for the turbulent fluctuation frequency 160 kHz. As it is seen in the figure, the imaginary part is much smaller than the real one; which is still finite at the ends of the probing interval. A very wide (lasting without decay till the reflectometry Bragg limit equal to 12 cm^{-1}) turbulence κ -spectrum (real and imaginary parts) obtained using procedures of [5] from the measured CCF is shown in Fig. 2. The accuracy of the spectrum reconstruction (estimated using the spectrum imaginary part and negative bursts of real part) is not high, but sufficient for the spectrum width estimation. It corresponds to the turbulence l_c substantially smaller than 0.5 cm. This estimation agrees qualitatively with the value of typical turbulence spatial scale obtained at FT-2 with enhanced scattering diagnostics [7] and provided for FT-2 by

$n_e(0) = (1.5 \text{ - } 3) \times 10^{13}$, $T_e = (200\text{-}500)$ eV), where a double antenna sets for O - and X -mode were installed both at high magnetic field sides. In the case of O -mode high field side probing in equatorial plane the signals CCF was measured with probing waves frequency difference step Δf varied by 0.1 GHz in the ± 4 GHz range, corresponding to

cutoffs spatial separation up to ± 1.5 cm. The

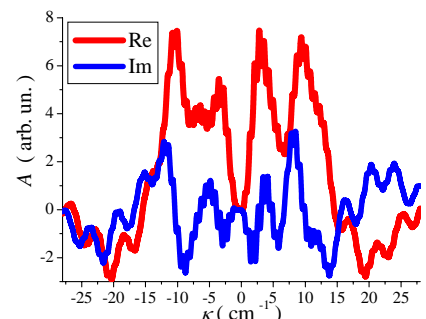


Fig. 2. Turbulence spectrums real and imaginary parts.

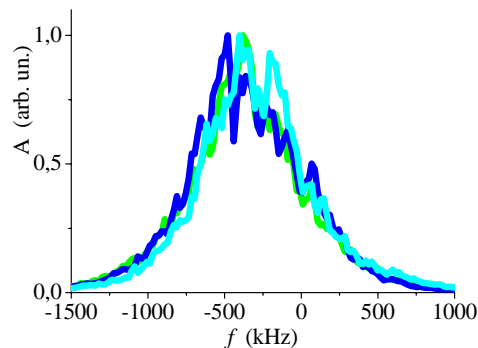


Fig. 3. Quadrature reflectometer spectra. The signal CCF was measured in the ± 3 GHz range (corresponding to cutoffs spatial separation up to ± 1.5 cm) with $\Delta f = 50$ MHz. The double antenna set was shifted out of the equatorial plane by 1.5 cm that corresponds to poloidal probing wave number of 3 cm^{-1} . The corresponding reflectometry (Doppler) spectrum shifted by 400 kHz from the probing frequency is shown in Fig. 3. The CCF absolute value (coherence) is shown in Fig. 4 to be finite only for cutoffs separation less than 0.5 cm. The signal correlation length is decreasing with growing turbulence frequency and reaches the value of 1 mm at 1.2 MHz. The coherence oscillations obvious at small turbulence frequencies are produced presumably by contribution of reflection at the plasma boundary to the fluctuation reflectometry signal. This explanation is supported by observation of component in the imaginary and real parts of the

ELMFIRe full-f gyrokinetic modeling [10] (see Fig. 8). Long-scale fluctuations are suppressed in the spectrum for $|\kappa| < 1 \text{ cm}^{-1}$, which is probably a shortcoming of the 1D model [5] used in the reconstruction procedure.

The spectrum decay at high wave numbers was studied with 60 GHz X-mode probing from the high magnetic

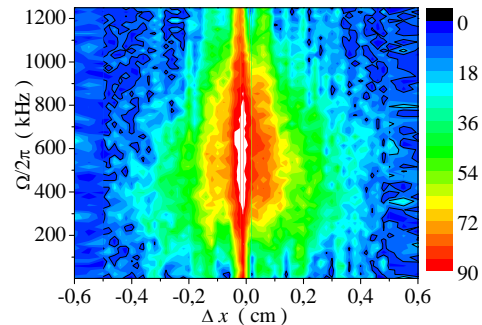


Fig. 4. CCF coherence.

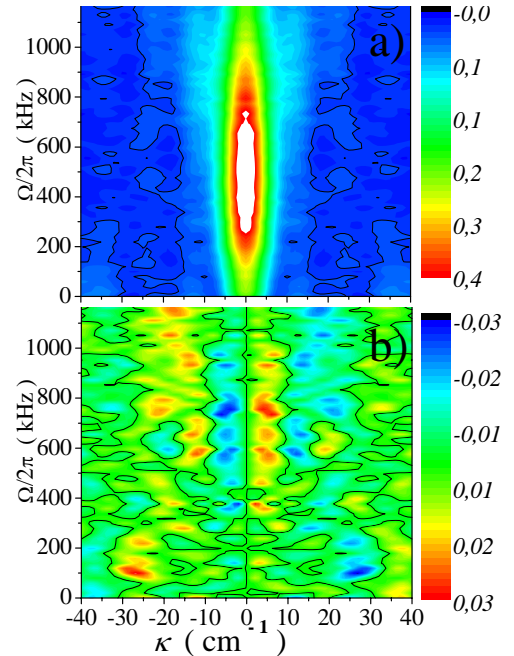


Fig. 5. CCS real and imaginary parts. correlation spectrum (CCS) at wave numbers $25-30 \text{ cm}^{-1}$ equal to the Bragg BS limit (see Fig. 5 a,b.) which is however much smaller than the dominant real part. Applying the expression (1) to these spectra we obtain the turbulence frequency and radial wave number spectrum shown in Fig. 6. The width of this spectrum is

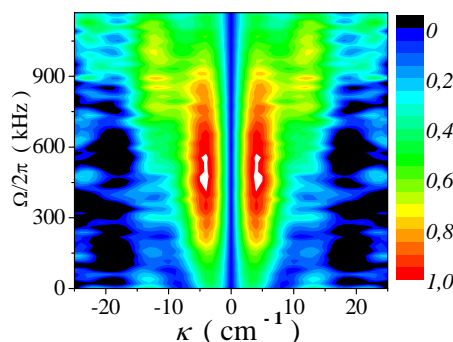


Fig. 6. Turbulence spectrum.

growing with the turbulence frequency demonstrating a clear dispersion. The suppression of the spectrum at very small wave numbers is most likely related to the limitations of the 1D model. The turbulent density fluctuation two-point correlation function is provided by the Fourier transform of the experimentally obtained spectrum (Fig. 6) in which only the contribution of physically sensible part within the Bragg limit is accounted for. The result of this transform is shown in Fig. 7. The turbulence CCF shown in Fig. 7 demonstrates decrease of the correlation length with growing frequency. This result of the turbulence wave number spectrum reconstruction based on the experimental RCR data is supported qualitatively by the properties of the density fluctuation CCF obtained as a result of full-f gyrokinetic global modeling for the 19 kA FT-2 discharge [10], but at 1.5 higher density, and shown in Fig. 8. It should be mentioned that very small correlation length values obtained numerically for turbulence frequency higher than 600 kHz are smaller than the computation grid and therefore not reliable.

Conclusion.

Summarizing the paper results, we emphasize the successful application of the turbulence wave number spectrum reconstruction procedure from the RCR data proposed in [5].

This work is partly supported by RF government grant 11.G34.31.0041 and RFBR grants 11-02-00561, 12-02-00515 and 12-02-09297-mob_z and by the Saint-Petersburg Government.

- [1] H. Hutchinson, Plasma Phys. Control. Fusion **34** 1225 (1992)
- [2] G. Leclert et al., Plasma Phys. Control. Fusion **48** 1389 (2006)
- [3] E.Z. Gusakov and A.Yu. Popov, Plasma Phys. Control. Fusion **44** 2327 (2002)
- [4] E.Z. Gusakov and A.Yu. Popov, Plasma Phys. Control. Fusion, **46** 1393 (2004)
- [5] E.Z. Gusakov and N.V. Kosolapova, Plasma Phys. Control. Fusion **53** 045012 (2011)
- [6] E.Z. Gusakov et al., Plasma Phys. Control. Fusion **42** 1033 (2000)
- [7] A.D. Gurevich et al., Nucl. Fusion **47** 245 (2007)
- [8] E.Z. Gusakov and B.O. Yakovlev, Plasma Phys. Control. Fusion **44** 2525 (2002)
- [9] N.V. Kosolapova, E.Z. Gusakov and S. Heuraux, Plasma Phys. Control. Fusion **54** 035008 (2012)
- [10] S. Leerink et al., this conference, P4.003 (2012)

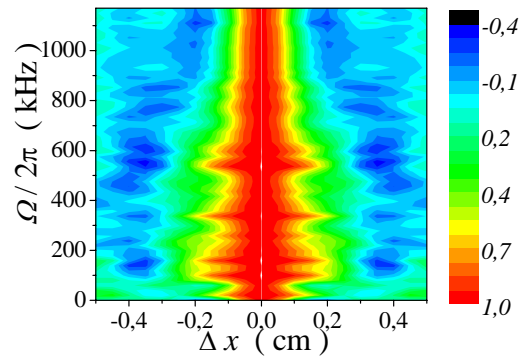


Fig. 7. Turbulence CCF reconstructed from measurements.

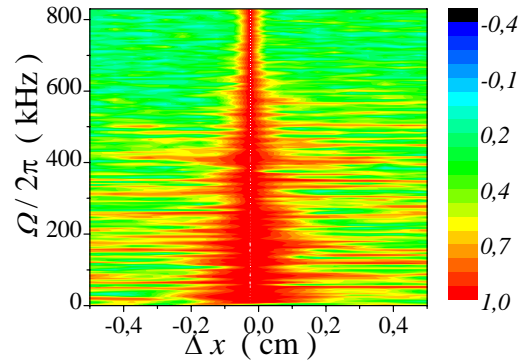


Fig. 8. Turbulence CCF, modelling.